Desalination and Water Treatment
www.deswater.com

doi: 10.5004/dwt.2017.0038

58 (2017) 106–119
January

Competitive adsorption of Cd (II) and Pb (II) ions from aqueous solution onto Iranian hematite (Sangan mine): optimum condition and adsorption isotherm study

Niyayesh Khorshidi, Amir Reza Azadmehr*

Department of Mining & Metallurgical Engineering, Amirkabir University of Technology, 424 Hafez Ave, Tehran, Iran, 15875-4413, Tel. +989308683038; email: nkh.explorer@aut.ac.ir (N. Khorshidi), Tel. +989124195819; email: a_azadmehr@aut.ac.ir (A.R. Azadmehr)

Received 10 January 2016; Accepted 30 May 2016

ABSTRACT

In the present study, Iranian hematite (from Sangan area, in the east of Iran) was characterized by XRD, XRF, and FTIR spectroscopies. Then, the efficiency of Iranian hematite for the removal of Pb (II) and Cd (II) ions from aqueous solution was investigated by the optimum condition (contact time, metal concentrations, pH of solutions and the amount of hematite) and equilibrium isotherm models. The Freundlich isotherm indicated a very good fit with the experimental data of Pb (II) and Cd (II) adsorption in an individual solution. In the binary solution, the obtained adsorption isotherm data showed fittings for Langmuir model (homogeneous adsorption mechanism) with the maximum adsorption capacity of 17.86 and 1.887 mg/g for Pb (II) and Cd (II), respectively. These results have been confirmed by three-parameter isotherm studies. The chemical absorption and particle diffusion are predominated for Pb (II) and Cd (II) adsorption in the binary solution, respectively. The competitive adsorption characteristics of Pb (II) and Cd (II) ions were approved by the extended Freundlich and extended Langmuir isotherm models, respectively. The antagonistic competitive effect was observed for the maximum adsorption capacity of Pb (II) and Cd (II) in the binary solution. Industrial wastewater contains many heavy metals, thus the use of natural adsorbents, such as raw hematite for simultaneous removal of Pb (II) and Cd (II) is an important issue.

Keywords: Hematite; Optimum condition; Competitive adsorption; Multi-component isotherms; Pb (II); Cd (II)

1. Introduction

Nowadays, environmental pollutants in different forms are discharged into nature. One of the major environmental pollutants is heavy metal contamination, which grows concerns because of health risk to animals and humans [1,2]. Cadmium and lead compounds are significant heavy metals which are used in various industries such as paint, plastics, rolled and extruded products, alloys, pigments, automotive and batteries [3]. They are toxic, and according to the United States Environmental Protection Agency (USEPA), the maximum acceptable concentration of cadmium and lead are 5 and 15 μg/L, respectively [4]. Consequently, cadmium through inhalation or contaminated drinking water causes irreparable damages to human [5]. Exposure to lead can hurt the central nervous system, cardiovascular system, reproductive system, blood system and kidney. Lead exposure increases the risk of cancer. These pollutants are left in the environment without any purification or filtration thus, before leaving in the environment, they must be filtrated [6].

Common methods for the removal of heavy metal ions from aqueous solutions mainly include chemical precipitation, ion exchange [2], coagulation and flocculation [3],

* Corresponding author.

Table 1
Concise summary of Pb (II) and Cd (II) adsorption on hematite

Adsorbent	Q_m(mg/g)	Kind of investigation	References
Iron ore slime (IOS) (Jindal Steel Ltd., Vijayanagaram, India)	63.57 mg/g Pb (II) and 34.75 mg/g Cd (II)	Isotherm, kinetic studies	[19]
Bog iron ores: the Polish Lowlands: Biadaszki (BI), DebeMałe (DM), Kolechowice (KOL) and Strzyzew (ST)	97.0, 25.2, 25.5, 55.0 mg/g for lead (II), copper (II), zinc (II), and chromium (III).	Optimum condition, isotherm studies	[20]
Natural hematite separated from natural ore (Chinese Central iron & Steel Research Institute)	0.185 mg/g Cu (II) and 0.552 mg/g Cd (II)	Isotherm studies	[21]
Iron ore slimes (an iron ore mine in Orissa, India)	9.5 mg/g Pb (II)	Optimum condition, isotherm studies	[22]
Iron oxide (hematite, α-Fe_20_3-H_20, 99.9%)	11.24 mg/g Cd (II)		[23]
Natural hematite (an iron ore from Noamundi mine, Bihar, India)	0.1225 mg/g Cd (II)	Optimum condition, isotherm studies, kinetic and thermodynamic studies	[24]

reversed osmosis and absorption [2]. Generally, these methods are expensive, thus developing low-cost methods is recommended. The adsorption process is one of the most efficient methods which is relatively easy handling and inexpensive [3]. Mineral adsorbents to remove heavy metals have attracted interest over the last two decades. The advantages of mineral adsorbents are their low cost and abundance in nature. Zeolite [7–9], bentonite [8–11], kaolinite [12–14] and magnetite [15,16] were used for the removal of Cd (II) and Pb (II) from industrial wastewater.

The wide range of environmental purification technologies and wastewater treatment have been developed to use iron compounds (special iron oxide) to clean up contaminated ground, surface and subsurface water [17]. One of the significant natural adsorbents is hematite (Fe_2O_3). The first report on the removal of heavy metals from aqueous solution by hematite was presented in 1992 [18].

As can be seen in Table 1 and according to the studies performed in recent years, many studies have reported the removal of heavy metals by using hematite. The literature survey shows that hematite can offer a potential adsorption method for the removal of Pb (II), Cd (II), Cu (II), Zn (II) and Cr (III) from wastewater. The sequence of the maximum adsorption capacity of heavy metals on hematite (natural Fe_2O_3) follows as Pb (II) > Cr (III) > Cd (II) > Zn (II) > Cu (II).

The best adsorbent for Pb (II) adsorption was bog iron ores (Fe_2O_3 = 70. 96%), and for Pb (II) and Cd (II) adsorption was iron ore slime (Fe_2O_3 = 86%) obtained from India (Vijayanagaram area) [19,20]. Despite these studies, the competitive adsorption of Pb (II) and Cd (II) on hematite has been disregarded. However, Iranian hematite has not yet been studied well for the competitive adsorption of heavy metals. In this study, Iranian hematite has been characterized by X-ray diffraction (XRD), X-ray fluorescence (XRF), and Fourier transform infrared spectroscopy (FTIR) to find chemical, physical and mineralogical properties, then optimum conditions of Pb (II) and Cd (II) adsorption on hematite and isotherm models (two and three parameters, extended and modified) have been determined.

2. Theory

2.1. Mono-component isotherm equations

Various isotherm equations (two-parameter and three-parameter) which were represented in Table 2 have been used to describe the equilibrium characteristics of adsorption.

2.2. Multi-component isotherm equations

Various isotherm equations such as the extended Freundlich and Langmuir, and modified Freundlich and Langmuir equations have been applied to describe the equilibrium characteristics of multi-component adsorption. These isotherm equations are given in Table 3.

3. Experimental

3.1. Material

A representative sample of hematite from the Sangan region in the east of Iran was used without any chemical pretreatment and modification in the adsorption studies. The sample was crushed to sizes below 150 microns by a ball mill. X-ray diffraction (XRD) and X-ray fluorescence (XRF) were used to characterize the mineralogy of hematite and its elemental analysis.

3.2. Physical measurements

XRD spectrum and XRF were obtained by using a Philips X-ray diffract meter 1,140 and a Philips X-ray diffract meter X unique II, respectively. Fourier transform infrared (FTIR)

Table 2
Equations of two parameter and three parameter isotherm models

Models	Equation	Descriptions	References
Two parameters			
Langmuir	$\frac{C_e}{q}=\frac{1}{Q_0\times b}+\frac{C_e}{Q_0}$ $R_L=\frac{1}{1+bC_0}$	q (mg/g): amount of adsorbed metal ion per unit weight of hematite. C_e (mg/L): metal ion concentration in solution at equilibrium (after adsorption). b (L/mg): the Langmuir isotherm constants Q_0: adsorption capacity, maximum in monolayer adsorption. R_L: separation factor also called equilibrium parameter	[25–26]
Freundlich	$\log q_e=\log K_f+\frac{1}{n}\log C_e$	K_F ($mg^{1-1/n}L^{1/n}g^{-1}$): Freundlich constants which display adsorption capacity of the hematite n (g/L): Freundlich constants which represent adsorption intensity (or surface heterogeneity) of the adsorbent	[25, 27]
Temkin	$q_e=\frac{RT}{b^{LnA}}+\frac{RT}{b^{LnC_e}}$	b (J/mol): Temkin isotherm constants that related to the heat of adsorption A: Temkin isotherm constants. R: The gas constant (8.314 J/mol K) T: The absolute temperature	[28, 29]
Dubinin-Radushkevich	$\mathrm{Lnq}=\mathrm{Lnq_{max}}-\beta R^2T^2\mathrm{Ln}^2(1+\frac{1}{C})$ $E=\frac{1}{\sqrt{2\beta}}$	q_{max} (mg/g): capacity maximum of adsorption β (mol^2/KJ^2): a constant related to adsorption energy E: free energy per molecule of adsorbate (KJ) which represent: • If E < 8 kJ/mol : physical adsorption • If 8 < E <16 kJ/mol : chemical absorption or ion exchange For E > 16 kJ/mol : particle diffusion governs the reaction	[30, 31]
Three parameter			
Khan	$q_e=\frac{q_m b_K C_e}{(1+b_K C_e)^{aK}}$	b_k and q_m: the Khan model constant a_k: the Khan model exponent q_e (mg/g) : equilibrium adsorption capacity C_e (mg/L): equilibrium concentration if $a_k \le 1$, it turns to Langmuir isotherm if $a_k > 1$ it tends to Freundlich model	[32]
BET	$q_e=\frac{q_s C_{BET} C_e}{(C_s-C_e)\left[1+(C_{BET}-1(C_e/C_s)\right]}$	C_{BET} (L/mg): the BET adsorption isotherm C_s (mg/L): adsorbate monolayer saturation concentration q_s (mg/g): theoretical isotherm saturation capacity	[25]
Koble–Corrigan	$q_e=\frac{AC_e^n}{1+BC_e^n}$	A ($L^n mg^{1-n}/g$), B $(L/mg)^n$ and n : the Koble–Corrigan isotherm constant n_k = 1 Langmuir form	[33–35]
Toth	$q_e=\frac{K_T C_e}{(a_T+C_e)^{1/t}}$	K_T (mg/g) and a_T (L/mg): Toth isotherm constant t: the Toth model exponent	[36, 37]
Redlich–Peterson	$q_e=\frac{K_R C_e}{1+a_R C_e^g}$	K_R (L/g) and a_R (L/mg): Redlich–Peterson isotherm constant g : Redlich–Peterson isotherm exponent g = 1 Langmuir form g = 0 Henry's law form	[25, 34, 35]

Table 3
Multi-component isotherm models and their description

Models	Equation	Descriptions	References
Modified Langmuir isotherm	$q_{e,i} = \frac{q_{m,i} K_{L,i} \left(C_{e,i} / \eta_i \right)}{1 + \sum_{j=1}^{N} K_{L,j} \left(C_{e,j} / \eta_j \right)}$	η_i: an interaction term and depends on the concentrations of the other components in the solution	[38, 39]
Extended Langmuir isotherm	$q_{e,i} = \frac{q_{\max} K_i C_{e,i}}{1 + \sum_{j=1}^{N} K_j C_{e,j}}$	q_{max}: the constant in extended Langmuir isotherm (mg/g) K_i: the individual extended Langmuir isotherm constant of each component (l/mg)	[38, 39]
Sheindorf–Rebuhn–Sheintuch (SRS) model	$q_{e,i} = K_{F,i} C_{e,i} \left(\sum_{j=1}^{N} a_{ij} C_{e,j} \right)^{(1/n_i) - 1}$	The constant $K_{F,i}$ and the exponent n_i are determined from the single-component equilibrium adsorption data a_{ij}: the competition coefficients which describe the inhibition to the adsorption of component i by component j	[38, 39]
Extended Freundlich isotherm	$q_{e,1} = \frac{K_{F,1} C_{e,1}^{n_1 + x_1}}{C_{e,1}^{x_1} + y_1 C_{e,2}^{z_1}}$ $q_{e,2} = \frac{K_{F,2} C_{e,2}^{n_2 + x_2}}{C_{e,2}^{x_2} + y_2 C_{e,1}^{z_2}}$	(x_1; y_1; z_1 and x_2; y_2; z_2): the multi-component Freundlich adsorption constants of the first and the second components.	[38, 39]

spectroscopy has been used for chemical functional groups. FTIR spectra from 4,000 to 400 cm^{-1} were recorded on a Shimadzu FTIR instrument, using KBr pellets. The concentration of lead and cadmium solution after adsorption was determined by the use of atomic absorption spectrometry of Unicam 939.

3.3. Optimum condition and adsorption isotherm experiments

The Pb (II) and Cd (II) adsorption experiments were carried out using a batch equilibrium method. All of the adsorption experiments were conducted in a 250.0 ml glass reactor using a shaker for mixing at ambient temperature. In this study, the influence of the parameters, such as the mass of hematite from 50.00 to 80.00 g/L, initial Pb (II) and Cd (II) concentration from 100.0 to 1,000.0 ppm, contact time from 15 to 120 min, and pH from 2.40 to 7.10 were investigated, and the optimized conditions for maximizing Pb (II) and Cd (II) adsorption were determined. The pH of the solution was adjusted with NaOH and HCl. All the other parameters were held constant for the investigation of each parameter in each test.

For single and binary metal system, the two-parameter (Langmuir, Freundlich, Temkin, and Dubinin–Radushkevich (D–R)), three-parameter (Khan, BET, Koble–Corrigan, Toth, Redlich–Peterson), Extended and Modified adsorption isotherm models were studied using 5 g of hematite added to 100 ml of solution containing different concentrations of each metal ion, ranging from 100.0 to 1,000.0 ppm. The mixtures were agitated at 600 rpm for 1 h in a shaker. All of the solutions were immediately filtered by a paper filter after each test.

4. Results and discussions

4.1. Characterization of raw hematite

The chemical analysis was performed using XRF spectrometry and the data were presented in Table 4. Fig. 1 shows the XRD pattern of raw hematite. This mineralogical study reveals that the main constituent of the sample is hematite, and impurity compounds are goethite, maghemite, and quartz which were confirmed by XRF and FTIR. The diffraction peaks at 33.4° 2-Theta indicate (104) planes of hematite mineral. The other diffraction peaks observed at 35.1° and 21.3° 2-Theta are related to (110) and (119) planes for maghemite and goethite minerals, respectively.

The FTIR spectrum of the raw hematite is illustrated in Fig. 2. In addition, the main vibrational modes of FTIR spectra have been summarized in Table 5. The broad-stretching band at 3426 cm^{-1} is concerned with an H–O–H stretching band of water molecules within the crystal structure of hematite. This broad band is due to hydrogen bonding between hydrogen and oxygen of different water molecules [40]. The broad band

Table 4
Chemical analysis of raw hematite sample (XRF data)

Samples	Fe_2O_3	SiO_2	CaO	MgO	Al_2O_3	Na_2O	K_2O	SO_3	MnO
Wt%	78. 3	9. 9	3.44	2.05	1. 29	0. 33	0.21	0.20	0.116

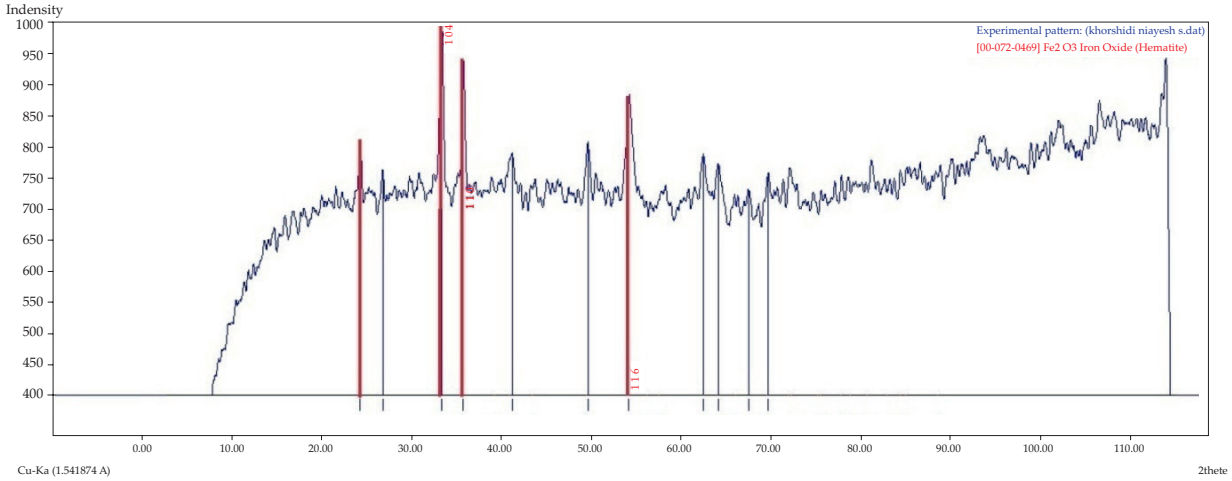

Fig. 1. X-ray diffraction of hematite.

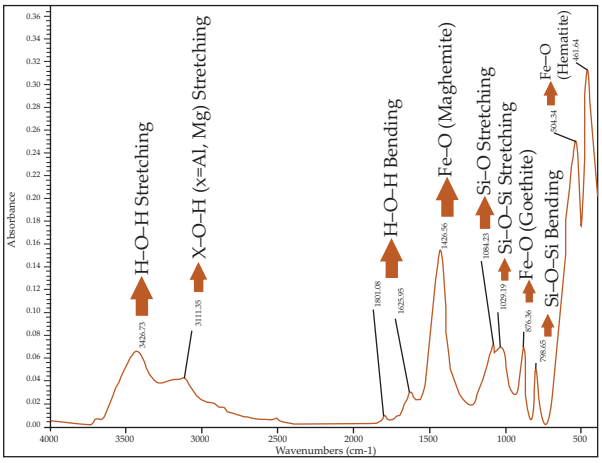

Fig. 2. FTIR spectra of raw hematite.

Table 5
The main vibrational modes of FTIR spectra of raw hematite

Assignment	Raw hematite (cm^{-1})
(H–O–H)	3426
(X–O–H), X = Al, Mg	3111
σ (H–O–H)	1625
Fe-O	1426
(Si–O)	1084
Si–O–Si	1029
Fe-O	876
σ Si–O–Si	798
Fe-O	540–461

at 3,111 cm^{-1} indicates the O–H band linkage of a hydroxyl group which interacts with Mg and Al atoms (Mg–OH and Al–OH) [41,42]. The bands at 1,426, 876 and 540–461 cm^{-1} are related to Fe–O functional group for maghemite, goethite, and hematite, respectively. It seems that the majority of the sample is hematite due to the high intensity of hematite bands [43]. The stretching and bending vibrations of Si–O–Si bands are observed at 1029 and 798 cm^{-1}, respectively. This proves the presence of quartz impurity in hematite sample.

4.2. Optimum conditions of Pb (II) and Cd (II) adsorption

4.2.1. Effect of mass of hematite

In order to study the effect of hematite quantity on the removal of Cd (II) and Pb (II) from aqueous solution, experiments were conducted with weights of 10.00–80.00 g/L, with 1000 mg/L Cd (II) and 1000 mg/L Pb (II) concentration at 25°C, a stirring speed of 600 rpm, and a particle size of –150 μm. Fig. 3 presents the results of Cd (II) and Pb (II) adsorption with different hematite values. The increase of adsorbent to liquid ratio causes the percentage of adsorption to increase to a maximum value at 80.0 g/L of hematite, so that the amount of available surface sites for ion exchange increases with the increasing mass of hematite [44]. This increase for Pb (II) (46.5%–88.1%) is more than Cd (II) (7.5%–18.4%). It is obvious that the dependence of the Pb (II) adsorption percentage to the mass of hematite is more than Cd (II) adsorption percentage.

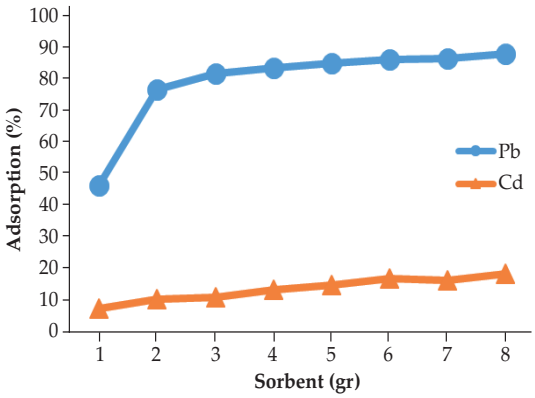

Fig. 3. The results of Cd (II) and Pb (II) adsorption with different hematite values, Pb (II) and Cd (II) = 1000 ppm, adsorbent = 10.00–80.00 g/L hematite, t = 1 h, stirring speed = 600 rpm.

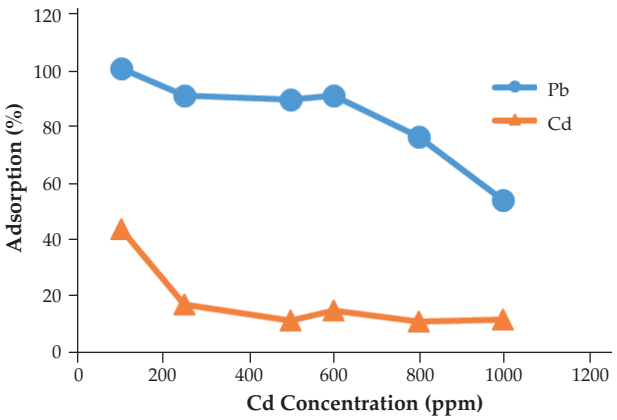

Fig. 6. Effect of initial Cd (II) concentration on Cd (II) and Pb (II) removal, adsorbent = 50 g/L, Pb (II) = 250 ppm, stirring speed = 600 rpm.

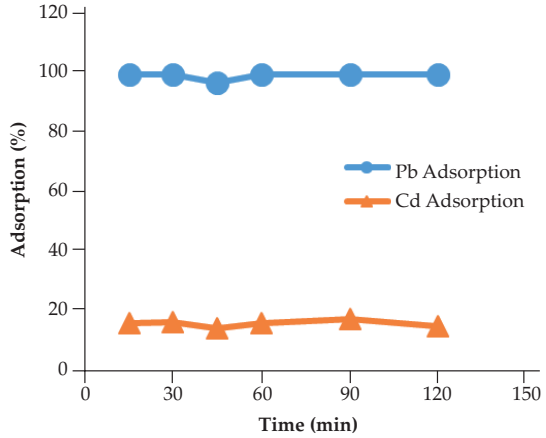

Fig. 4. The results of Cd (II) and Pb (II) adsorption versus time in binary system, Pb (II) = 1000 ppm, Cd (II) = 250 ppm, adsorbent = 50 g/L, stirring speed = 600 rpm.

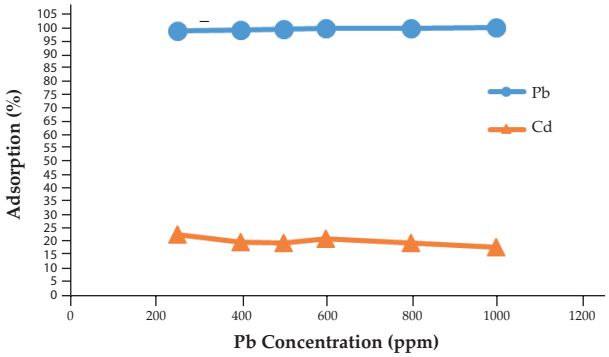

Fig. 7. Effect of initial Pb (II) concentration on Cd (II) and Pb (II) removal, adsorbent = 50 g/L, Cd (II) = 250 ppm, t = 1 h, stirring speed = 600 rpm.

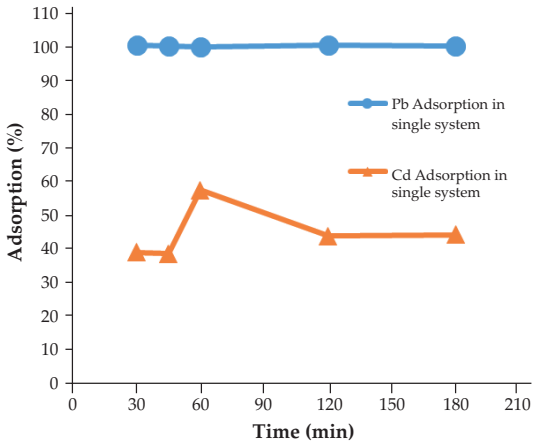

Fig. 5. The results of Pb (II) and Cd (II) versus time in single system, Pb (II) = 1000 ppm, Cd (II) = 250 ppm, adsorbent = 50 g/L, stirring speed = 600 rpm.

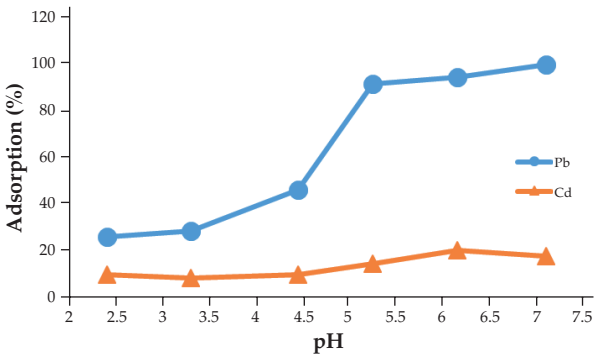

Fig. 8. Effect of pH on adsorption of Cd (II) and Pb (II), Pb (II) and Cd (II) = 1000 ppm, adsorbent = 50 g/L, t = 1 h, stirring speed = 600 rpm.

4.2.2. Effect of contact time

The effect of contact time on the adsorption of Cd (II) and Pb (II) onto hematite in the binary solution was investigated using a constant concentration of 1000 mg/L Pb (II) and 250 mg/L Cd (II), a particle size of hematite of –150 μm at room temperature (Fig. 4). Different contact times from 15 to 120 min were studied for the adsorption of Cd (II) and Pb (II) onto hematite. After passing 15 min from adsorption process initiation, the adsorption of Pb (II) ions reached to the maximum amount of adsorption (99.23%) and with the increase of contact time, Pb (II) adsorption was almost constant, but the increase of Cd (II) adsorption value from 15 to 90 min contact time was not obviously observed. This phenomenon is related to the large radius size of Cd (II) ion [44]. As seen in Fig. 5, in a single solution, the adsorption of Pb (II) is high for all contact times (more than 99%), but the maximum uptake of Cd (II) occurred at $t = 60$ min (57.2%), therefore this contact time is chosen for the optimum condition.

4.2.3. Effect of initial concentration effect of initial Cd (II) concentration on Cd (II) and Pb (II) removal

The adsorption of Cd (II) and Pb (II) onto hematite was studied at different initial concentrations of Cd (II) ranging from 100 to 1,000 mg/L at a ratio of mass of hematite to liquid (m/V) of 50 g/L, a particle size of –150 μm/L and constant concentration of Pb (II). The Cd (II) and Pb (II) removal percentages decreased with increasing initial Cd (II) concentrations. This shows that Cd (II) uptake was limited to active hematite adsorption sites.

4.2.4. Effect of initial Pb (II) concentration on Cd (II) and Pb (II) removal

The adsorption of Cd (II) and Pb (II) onto hematite was studied at different initial concentrations of Pb (II) ranging from 250 to 1,000 mg/L at a ratio of mass of hematite to liquid (m/V) of 50 g/L, a particle size of –150 μm/L and constant concentration of Cd (II). As can be seen in Fig. 7, the increasing initial concentration of ions decreases the removal efficiency for Cd (II) ions. This phenomenon can be ascribed to the fact that there are no available adsorption sites for the extra ions at a constant amount of the adsorbent; however, the adsorption of Pb (II) ion due to its small radius is high for all concentrations [44].

4.2.5. Effect of pH on adsorption of Pb (II) and Cd (II)

The influence of pH was investigated at ambient temperature and a solid to liquid ratio of 50.00 (g/L), over a pH range of 2.40–7.10. The pH was adjusted by adding 0.1 M HCl and 0.1 M NH_3. Based on other related studies, it is found that at pH < 5.0, Pb (II) and Cd (II) species are totally present in ionic states. By increasing pH, Pb (II) and Cd (II), species start to hydrolyze ($Pb(OH)^+$) and they entirely precipitate into $Pb(OH)_2$ at pH > 6.0, whereas the formation of $Cd(OH)_2$ starts at pH > 8 [45]. Fig. 8 shows that the adsorption percentage of Pb (II) has increased from pH 2.40 to 7.10 while no significant effect on Cd (II) adsorption was observed. This result could be interpreted that in pH higher than 6, Pb (II) has precipitated as $Pb(OH)_2$. In other words, the removal of Cd (II) in the presence of Pb (II) is not enhanced with increasing pH; therefore, Pb (II) ion is an inhibitor factor for increasing Cd (II) removal value [46–48].

4.3. Single and binary adsorption of Cd (II) and Pb (II) ions

4.3.1. Single-component adsorption isotherm of Pb (II) and Cd (II) adsorption

A number of experiments were performed to evaluate two-, and three -parameter adsorption equilibrium isotherm models based on the various concentrations of metal ions. Two-parameter models (Langmuir, Freundlich, Temkin and Dubinin–Radushkevich) were fitted by the linear form of equations and their parameters were calculated by the linear regression. MATLAB software was employed for the determination of the constants of three -parameter models. The isotherm parameters for each metal ion are listed in Tables 6 and 7.

4.3.1.1. Two-parameter models

As observed in Fig. 9, Langmuir and Freundlich isotherm models for Pb (II) and Cd (II) adsorption are plotted. In a single system, the Freundlich model with correlation coefficient $R^2 = 0.994$ and $R^2 = 0.979$ for Pb (II) and Cd (II) respectively fits the experimental data better than the Langmuir, Temkin and D-R models, which implies that the adsorption of metal ions onto hematite is heterogeneous. According to Table 6, the values of exponent n for Pb (II) and Cd (II) are 0.869 and 1.355, respectively. With respect to these values, the lower value of the exponent n signifies a higher affinity and the heterogeneity of the adsorbent sites [49].

The values of Pb (II) and Cd (II) adsorption capacity which were calculated from the Langmuir model are 47.619 and 13.699 mg/g, respectively.

According to the D-R model, the calculated adsorption free energy (E) indicates that either the chemical absorption or ion exchange governs the adsorption process of Pb (II) and Cd (II) ions onto hematite.

4.3.1.2. Three-parameter models

The correlation coefficient (R^2) and the parameters of Khan, BET, Koble–Corrigan, Toth and Redlich–Peterson models are mentioned in Table 7. The sequence of isotherm models considering R^2 values for Pb (II) ion is in this order: BET > Khan > Koble–Corrigan > Redlich Peterson. In other words, BET model exhibits the best fit with a correlation coefficient ($R^2 = 0.973$) for Pb (II) adsorption on hematite. The C_{BET} value (2.574 L/mg), which is relevant to bending energy, indicates the strong interaction and is dominant between adsorbent and adsorbate. With respect to the constant n value of Koble-Corrigan model and g value of Redlich–Peterson model which approach to zero, it is proved that Pb (II) adsorption mechanism is heterogeneous.

The sequence of isotherm models for Cd (II) ion is predominant: Koble–Corrigan > Khan > Toth > Redlich Peterson > BET. Cd (II) adsorption has a good correlation coefficient (R^2=0.961) with Koble-Corrigan model. The constant n is close to zero, indicating that the equilibrium isotherm model is approaching to the Freundlich equation.

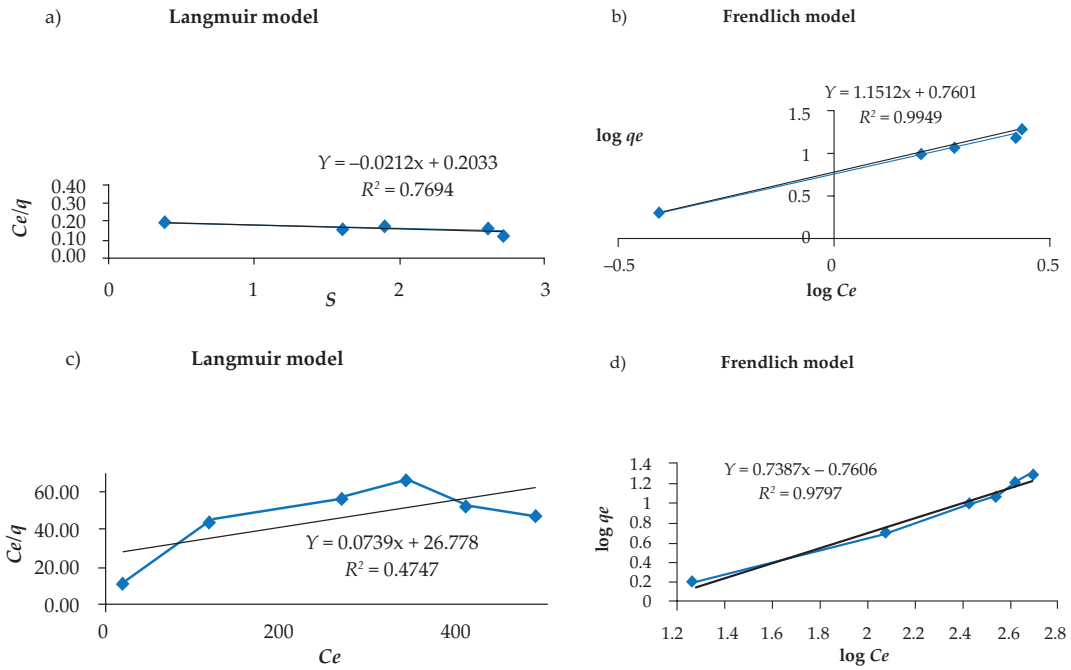

Fig. 9(a) and (b) Langmuir and Freundlich isotherm models for Pb (II) adsorption on raw hematite. (c) and (d) Langmuir and Freundlich isotherm models for Cd (II) adsorption on raw hematite.

Table 6
Langmuir, Freundlich, Temkin, and Dubinin–Radushkevich isotherm constants for lead and cadmium adsorption

Model	Parameter	Pb	Cd
Langmuir	R^2	0.769	0.474
	Q_0 (mg/g)	47.619	13.699
	b	0.1034	2.727×10^{-3}
	SD	0.069	0.50
Freundlich	R^2	0.994	0.979
	n (g/L)	0.869	1.355
	K_F ($mg^{1-1/n}L^{1/n}g^{-1}$)	5.754	5.754
	SD	0.029	0.10
Temkin	R^2	0.885	0.658
	b (j/mol)	307.1	1183.7
	A (L/mg)	2.862	14.576
	SD	0.290	0.49
Dubinin–Radushkevich	R^2	0.994	0. 826
	β (mol^2/ Kj^2)	7.66×10^{-9}	5.70×10^{-9}
	E (KJ)	8.081	9.364
	SD	0.007	0.03

Of course, the constant g value of Redlich–Peterson model confirms heterogeneous adsorption [38,39].

4.3.2. Multicomponent adsorption models

The simultaneous adsorption data of Cd (II) and Pb (II) from the binary system have been fitted to the multicomponent isotherm models. The parametric values of all the multicomponent adsorption models are given in Tables 8 to 11.

4.3.2.1. Two-parameter models in binary solution

According to Fig. 10 and Table 8, the Langmuir isotherm fits the experimental data better than other models, which implies that homogeneous adsorption of Pb (II) and Cd (II) on the surface of hematite has occurred. In other words, all absorptive sites interact with Pb (II) and Cd (II) ions with equal energies. The Langmuir isotherm model shows that the b value of Pb (II) ion is higher than that of Cd (II) ion, indicating that the adsorption energy of Pb (II) ion is higher than Cd (II) ions [50]. The maximum adsorption capacity value for Pb (II) ions (Q_{max} = 17.86 mg/g) on hematite is more than that for Cd (II) ions (Q_{max} = 1.887 mg/g). This is according to the size of metal ions which Pb (II) (1.54 Å) < Cd (II) (1.61 Å) and the electronegativity of Pb (II) (2.33) is more than that for Cd (II) (1.69). This phenomenon is due to the fact that smaller and more electronegative metal ions have a better availability to the functional group of surface and pores than the bigger and less electronegative metal ions, causing the higher adsorption capacity of the smaller metal ions [49–52].

Compared with the single system, the Q_{max} values of Pb (II) and Cd (II) ions in the Langmuir model decrease in binary systems, as the Q_{max} of Pb (II) in the single system decreased from 47.62 to 17.86. This result indicates that there

Table 7
Khan, BET, Koble–Corrigan and Toth isotherm constants for lead and cadmium adsorption

Model	Parameter	Pb	Cd
Khan	R^2	0.971	0.925
	q_m (mg/g)	6.85	1.081
	b_k	0.676	0.007
	a_k	0.368	0.639
BET	R^2	0.973	0.793
	q_s mg/g	13.714	3.875
	C_S mg/L	5.652	829.95
	C_{BET} L/mg	2.574	1339
Koble–Corrigan	R^2	0.958	0. 961
	A ($L^n mg^{1-n}/g$)	1.369	0.354
	B $(L/mg)^n$	0.778	0.226
	n	0.161	0.216
Toth	R^2	–	0.891
	a_T (L/mg)	–	11797
	K_T (mg/g)	–	0.019
	t	–	25411
Redlich–Peterson	R^2	0.942	0.887
	a_{RP} (L/mg)	10.905	0.147
	K_{RP} (L/g)	6.591	0.024
	g	–81.861	0.120

Table 8
Langmuir, Freundlich, Temkin, and Dubinin–Radushkevich isotherm constants for lead and cadmium adsorption

Model	Parameter	Cd	Pb
Langmuir	R^2	0.976	0.989
	Q_0 (mg/g)	1.887	17.86
	b	0.036	0.062
	R_L	0.027–0.22	0.016–0.14
	SD	0.15	0.34
Freundlich	R^2	0.650	0.909
	n (g/L)	6.80	2.37
	K_F ($mg^{1-1/n}L^{1/n}g^{-1}$)	1.42	2.21
	SD	0.25	0.24
Temkin	R^2	0.576	0.960
	b (j/mol)	11060	825
	A (L/mg)	5.50	1.27
	SD	0.13	0.13
Dubinin–Radushkevich	R^2	0.659	0.931
	β (mol^2/ Kj^2)	1.79×10^{-9}	3.58×10^{-9}
	E (KJ)	16.703	11. 81
	SD	0.012	0.02

is a competition among the Pb (II) and Cd (II) adsorption on hematite.

The R_L of hematite is 0.016–0.14 and 0.027–0.22 for initial concentrations of Pb (II) and Cd (II) between 100 and 1,000 ppm, respectively. This data shows Pb (II) and Cd (II) adsorption onto hematite from binary solution in different concentrations, which is favorable and reversible because $0 < R_L < 1$.

The adsorption free energy (E) value of Cd (II) adsorption in the presence of Pb (II) ions indicates that particle diffusion has dominated the Cd (II) adsorption process. In contrast, the mechanism of Pb (II) adsorption in the presence of Cd (II) is a chemical absorption or ion exchange.

4.3.2.2. Three-parameter models in binary solution

As seen in Table 9, the adsorption process of Pb (II) ions in the presence of Cd (II) ions is fitted appropriately with Redlich-Peterson, Toth and Khan isotherm models.

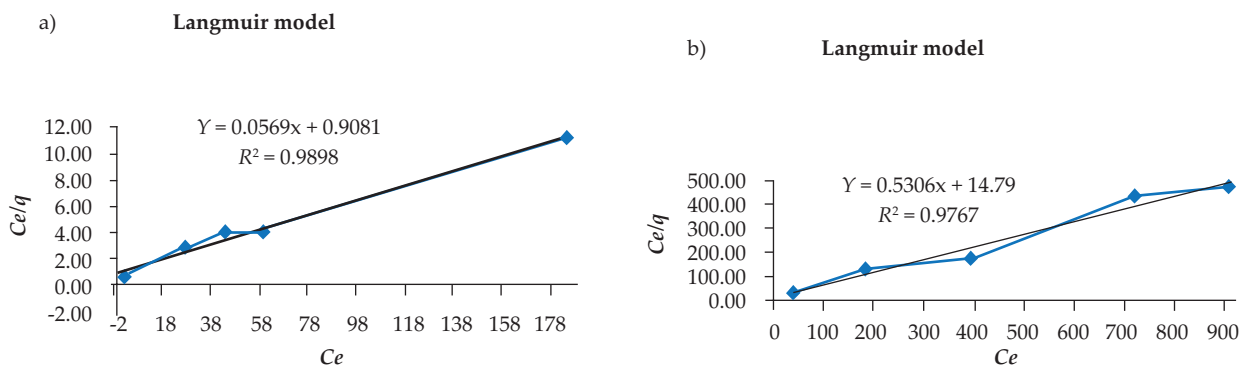

Fig. 10(a) Langmuir isotherm models for Pb (II) adsorption on raw hematite. (b) Langmuir isotherm models for Cd (II) adsorption on raw hematite.

Table 9
Khan, BET, Koble–Corrigan and Toth isotherm constants for lead and cadmium adsorption

Model	Parameter	Pb	Cd
Khan	R^2	0.9577	0.579
	q_m (mg/g)	7.71	1.393
	b_k	0.276	0.081
	a_k	0.800	0.926
BET	R^2	0.381	–
	q_s mg/g	6.189	–
	C_S mg/L	13.059	–
	C_{BET} L/mg	0.956	–
Koble–Corrigan	R^2	0.835	0. 590
	A ($L^n mg^{1-n}/g$)	0.550	0.333
	B $(L/mg)^n$	0.889	0.154
	n	0.016	0.557
Toth	R^2	0.9577	0.579
	a_T (L/mg)	3.618	12.337
	K_T (mg/g)	5.96	1.158
	t	1.250	1.079
Redlich–Peterson	R^2	0.958	–
	a_{RP} (L/mg)	0.347	–
	K_{RP} (L/g)	2.413	–
	g	0.825	–

According to g value of Redlich-Peterson model which is 0.825, the Pb (II) adsorption process in the binary solution onto hematite is described by Langmuir equation [38,39].

With respect to constant a_k in the Khan model for Pb (II) adsorption in the presence of Cd (II) (a_k = 0.80) which approaches to unity, the Khan model turns into Langmuir isotherm model.

Similar to Redlich-Peterson and Khan isotherm models, Toth model turns into Langmuir model because constant t value in this model is limited to unity [36]. Consequently, Redlich-Peterson, Khan and Toth models confirm the Langmuir model.

Although a reasonable correlation coefficient (R^2) is not found for Cd (II) adsorption on the three-parameter isotherm models, the constant a_k in the Khan model for Cd (II) adsorption in the presence of Pb (II) (a_k = 0.926) supports the view that adsorption process onto hematite is described by homogeneous mechanism.

4.3.2.3. Extended and modified isotherm models in binary solution

The multi-component isotherms, including modified Langmuir isotherm, extended Langmuir isotherm, Sheindorf–Rebuhn–Sheintuch model (SRS; modified Freundlich), and extended Freundlich isotherm were used to fit the binary sorption data. The parameters values of the models are represented in Tables 10 and 11 below. To determine the parameters of all these multi-component models, the MATLAB software was employed. The MPSD (Marquardt's percent standard deviation) values between the experimental and calculated q_e values is given as: [49]

$$\mathrm{MPSD} = 100\sqrt{\frac{1}{n_m - n_p}\sum_{i=1}^{n}\left(\frac{(\sum_{i=1}^{N} q_{e,i,\exp}) - (\sum_{i=1}^{N} q_{e,i,cal})}{(\sum_{i=1}^{N} q_{e,i,\exp})}\right)_i^2}$$

According to Tables 10 and 11, the multi-component modified Freundlich model shows a poor fit to the experimental data for both metal ions (MPSD = 96 and 36.8 for Pb (II) and Cd (II), respectively). Of course, the modified Langmuir model could not well describe experimental data since its MPSD for Cd (II) and Pb (II) ions are 48.6 and 44.1, respectively. The extended Langmuir and the extended Freundlich models fitted into the binary adsorption data of Cd (II) onto hematite reasonably well. However, the extended Langmuir model best fitted the experimental data with the lowest MPSD value of 23.8 in comparison with extended Freundlich (MPSD = 24.5). The comparison of the values obtained for q_{max} of Cd (II) adsorption from extended Langmuir model (1.572 mg/g) with the obtained q_{max} values from Langmxuir model in the single system (13.699 mg/g) showed that there is a competition between Cd (II) and Pb (II) in homogeneous adsorption onto binding sites of hematite which limits adsorption process and decreases maximum adsorption capacity of Cd (II) [38,39,49]. Consequently, the presence of Pb (II) causes Cd (II) adsorption to tend to homogenous adsorption from heterogeneous adsorption in individual solution.

According to the experimental data of Pb (II) adsorption in binary solution, the extended Freundlich model with the lowest MPSD value of 9.4 describes the adsorption mechanism better than other models. According to the extended Freundlich model, Pb (II) individually follows the heterogeneous adsorption and in the presence of Cd (II) ions, an exponential distribution of adsorption energies for Pb (II) adsorption is equivalent to the distribution in the single solution.

4.3.2.4. Evaluation of adsorption isotherm models of Pb (II) and Cd (II) onto hematite

The equilibrium data modelings of Pb (II) and Cd (II) adsorption in single and binary solution have been studied using two-parameter (Langmuir, Freundlich, Temkin, and Dubinin–Radushkevich (D–R)), three-parameter (Khan, BET, Koble–Corrigan, Toth, Redlich–Peterson), extended and modified adsorption isotherm models.

The Freundlich isotherm model is dominated in the individual solution of Pb (II) and Cd (II) ions by assuming a heterogeneous surface with the non-uniform distribution of energy binding of Pb (II) and Cd (II) adsorption on the hematite surface. Although experimental data of Pb (II) and Cd (II) ions in binary solution are in accordance with the Langmuir isotherm model, the adsorption mechanism is homogeneous.

In order to investigate the more characterization of Pb (II) and Cd (II) adsorption mechanism in the binary solution, modified Langmuir, modified Freundlich, extended Langmuir and extended Freundlich models have been studied (Table 12).

Based on marquardt's percent standard deviation error function, in Pb (II) adsorption, the extended Freundlich could describe the adsorption process better which demonstrates that the behavior of Pb (II) adsorption in the presence of Cd (II) is the same as that in the individual solution.

Table 10
Extended and modified isotherm models of Pb (II) adsorption in presence of Cd (II)

Langmuir model				Freundlich model		
Adsorbate	K_L	q_m	r^2	K_F	n	r^2
Pb	0. 062	17.86	0.989	2.21	2.37	0.909
Cd	0.036	1.887	0.976	1.42	6.80	0.650

Modified Langmuir model		Extended Langmuir model	
Adsorbate	η	K_i	q_{max}
Pb	1.3746	0.396	4.591
Cd	0.1356	–0.021	
MPSD	44.1	70.1	

Modified Freundlich model			Extended Freundlich model		
Adsorbate	a_{11}	a_{12}	x_i	y_i	z_i
Pb-Cd	–0.236	1.199	–0.98	57.6	-0.84
MPSD	96		9.4		

Table 11
Extended and modified isotherm models of Cd (II) adsorption in presence of Pb (II)

Langmuir model				Freundlich model		
Adsorbate	K_L	q_m	r^2	K_F	n	r^2
Pb	0. 062	17.86	0.989	2.21	2.37	0.909
Cd	0.036	1.887	0.976	1.42	6.80	0.650

Modified Langmuir model		Extended Langmuir model	
Adsorbate	η	K_i	q_{max}
Pb	2.9802	–0.066	1.572
Cd	3.6863	0.075	
MPSD	48. 6	23.8	

Modified Freundlich model			Extended Freundlich model		
Adsorbate	a_{21}	a_{22}	x_i	y_i	z_i
Pb-Cd	1.193	–0.183	–1.33	5.13	–0.06
MPSD	36.8		24.5		

The MPSD value of extended Langmuir model for Cd (II) adsorption in the presence of Pb (II) emphasizes that Langmuir model is the best model to represent the binary equilibrium isotherm data.

4.4. Mutual interference effects of metal ions on adsorption

A solution of different heavy metals usually shows three possible types of interactions: the first can be a synergism effect (i.e., the amount of adsorbed metal in the binary solution is greater than the amount of adsorbed metal in single solution $q'_e/q_e>1$), the second effect is antagonism (i.e., the amount of adsorbed metal in the binary solution is less than the amount of adsorbed metal in single solution $q'_e/q_e<1$), and the third is non-interaction (i.e., the heavy metals have no effect on the adsorption of each of the adsorbates in the solution) [49,53].

The q'_e/q_e ratios for the adsorption of one metal in the presence of another metal are shown in Table 13.

The q'_e/q_e ratios for Cd (II) and Pb (II) adsorption are less than unity, indicating that the adsorption of the metals was influenced by the presence of other metal ions in the binary system and there is an inhibitory effect of one metal on the binding of the other metal [53], hence the effect of Pb (II)

Table 12
Summaries of isotherm models

Metal ion	Single solution Two and three parameter	Binary solution Two and three parameter	Binary solution Extended and modified
Pb (II)	Freundlich and BET (heterogeneous)	Langmuir and Redlich-Peterson (homogeneous)	Extended Freundlich
Cd (II)	Freundlich and Koble–Corrigan (heterogeneous)	Langmuir (homogeneous)	Extended Langmuir

Table 13
Single and binary system adsorption parameters

System	Metal ion (+interferent)	$Q_{e,exp}$ (mg/g)	Q_{max} (mg/g)	Q'_e/Q_e	R^2
a) Pb as primary metal ion					
Single	Pb	15.95	Langmuir model	–	0.769
			47.619		
Binary	Pb-Cd	14.798	17.86	0.92	0.989
b) Cd as primary metal ion					
Single	Cd	7.74	Langmuir model	–	0.474
			13.699		
Binary	Cd-Pb	1.664	1.887	0.21	0.976

and Cd (II) on each other in binary solution is antagonistic. Interestingly, the maximum adsorption capacities of hematite for Pb (II) (17.86 mg/g) and Cd (II) (1.887 mg/g) in binary solution were lower than those of Pb (II) (47.619 mg/g) and Cd (II) (13.699 mg/g) ions alone.

According to Freundlich model, in single and binary solution (Tables 6 and 8) the value of K_f for Cd (II) and Pb (II) decreased in the presence of the secondary metal ion in the solution. A decrease in K_f by the secondary metal ion reflects the antagonistic interaction between metal ions for binding to the sites [54].

5. Conclusions

- Experimental data present that increasing the amount of hematite and the reduction of initial Pb (II) and Cd (II) concentration improves the removal efficiency of both metal ions in the presence of each other.
- Simultaneous adsorption of Cd (II) and Pb (II) is not dependent on time. By increasing pH from 2.40 to 7.10, the adsorption percentage of Pb (II) increased, while no significant effect on Cd (II) adsorption was observed.
- The Freundlich isotherm model shows a very good fit with the experimental data of Pb (II) and Cd (II) adsorption in an individual solution.
- In the binary Pb (II) and Cd (II) solution, the obtained adsorption isotherm data showed fittings for Langmuir model with maximum adsorption capacities of 17.86 and 1.887 mg/g for Pb (II) and Cd (II), respectively. Of course, the three-parameter isotherm studies confirmed the Langmuir isotherm which represents a homogeneous monolayer adsorption mechanism. The hypothesis adsorption mechanism for Pb (II) and Cd (II) in the binary solution is described by chemical absorption/ion exchange and particle diffusion, respectively.
- The competitive adsorption characteristics for Pb (II) and Cd (II) ions were approved by the extended Freundlich and extended Langmuir isotherm models, respectively. The antagonistic competitive effect was observed for two metals, which is relevant to the size and electronegativity of the metal ions.
- The maximum adsorption capacity of Pb (II) ratio to the maximum adsorption capacity of Cd (II) in single and binary solution are more than three (47.619/13.699) and nine (17.86/1.887), respectively. This obviously illustrates the appropriate selective adsorption of hematite for Pb (II) ions in the presence of Cd (II).
- This study introduces Iranian hematite as an appropriate and selective adsorbent for Pb (II) removal from aqueous solution.

References

[1] F. Fu, Q. Wang, Removal of heavy metal ions from wastewaters: A review, J. Environ. Manage., 92 (2011) 407–418.

[2] X.S. Wang, L. Zhu, H.J. Lu, Surface chemical properties and adsorption of Cu (II) on nanoscale magnetite in aqueous solutions, Desalination, 276 (2011) 154–160.

[3] P. Djomgoue, M. Siewe, E. Djoufac, P. Kenfack, D. Njopwouo, Surface modification of Cameroonian magnetite rich clay with Eriochrome Black T. Application for adsorption of nickel in aqueous solution, Appl. Surf. Sci., 258 (2012) 7470–7479.

[4] United States Environmental Protection Agency (USEPA) (1986). Quality Criteria for Water. EPA/ 440/5-86-001.

[5] G. Tan, D. Xiao Adsorption of cadmium ion from aqueous solution by ground wheat stems. J. Hazard Mater., 164(2–3) (2009) 1359–1363.

[6] M. Swapna, Applied Mineralogy Application in Industry and Environment, copublished by Springer, 2011.

[7] U. Wingenfelder, B. Nowack, G. Furrer, R. Schulin, Adsorption of Pb and Cd by amine-modified zeolite, Water Res., 39 (2005) 3287–3297.

[8] M. Hamidpour, M. Afyuni, M. Kalbasi, A.H. Khoshgoftarmanes, V. J. Inglezakis, Mobility and plant-availability of Cd (II) and Pb (II) adsorbed on zeolite and bentonite, Appl. Clay Sci., 48 (2010) 342–348.

[9] M. Hamidpour, M. Kalbasi, M. Afyuni, H. Shariatmadari, P.E. Holm, H. C. B. Hansen Sorption hysteresis of Cd (II) and Pb (II) on natural zeolite and bentonite, J. Hazard. Mater., 181 (2010) 686–691.

[10] S. Kozar, H. Bilinski, M. Branica, M. Schwuger, Adsorption of Cd (II) and Pb (II) on bentonite under estuarine and seawater conditions, Sci. Total Environ., 121 (1992) 203–216.

[11] G. Bereket, A.Z. Arog, M.Z. Özel, Removal of Pb (II), Cd (II), Cu (II), and Zn (II) from aqueous solutions by adsorption on bentonite, J. Colloid Interface Sci., 187 (1997) 338–343.

[12] E. Unuabonah, K. Adebowale, B. Olu-Owolabi, L. Yang, Comparison of sorption of Pb^{2+} and Cd^{2+} on kaolinite clay and polyvinyl alcohol-modified kaolinite clay, Adsorption, 14 (2008) 791–803.

[13] R.W. Puls, R.M. Powell, D. Clark, C. J. Eldred, Effects of pH, solid/solution ratio, ionic strength, and organic acids on Pb and Cd sorption on kaolinite, Water, Air, Soil Pollut., 57 (1991) 423–430.

[14] A. Sari, M. Tuzen, D. Citak, M. Soylak, Equilibrium, kinetic and thermodynamic studies of adsorption of Pb (II) from aqueous solution onto Turkish kaolinite clay, J. Hazard. Mater., 149 (2007) 283–291.

[15] Y. Mamindy-Pajany, C. Hurel, N. Marmier, M. Roméo, Arsenic (V) adsorption from aqueous solution onto goethite, hematite, magnetite and zero-valent iron: Effects of pH, concentration and reversibility, Desalination, 281 (2011) 93–99.

[16] A. Zach-Maor, R. Semiat, H. Shemer, Removal of heavy metals by immobilized magnetite nano-particles, Desal. Wat. Treat., 31 (2011) 64–70.

[17] A. Cundy, L. Hopkinson, R. Whitby, Use of iron-based technologies incontaminated land and groundwater remediation: A review, J. Sci. Total Environ., 400 (2008) 42 -51.

[18] S. Musić, M. Ristic, Adsorption of zinc (II) on hydrous iron oxides, J. Radioanal. Nucl. Chem., 162 (1992) 351–362.

[19] M. Mohapatra, K. Rout, B. Mohapatra, S. Anand, Sorption behavior of Pb (II) and Cd (II) on iron ore slime and characterization of metal ion loaded sorbent, J. Hazard. Mater., 166 (2009) 1506–1513.

[20] G. Rzepa, T. Bajda, T. Ratajczak, Utilization of bog iron ores as sorbents of heavy metals, J. Hazard. Mater., 162 (2009) 1007–1013.

[21] W. Li, S. Zhang, W. Jiang, X. Shan, Effect of phosphate on the adsorption of Cu and Cd on natural hematite, Chemosphere, 63 (2006) 1235–1241.

[22] L. Panda, B. Das, D.S. Rao, Studies on removal of lead ions from aqueous solutions using iron ore slimes as adsorbent, Korean J. Chem. Eng., 28 (2011) 2024–2032.

[23] A.P. Davis, V. Bhatnagar, Adsorption of cadmium and humic acid onto hematite, Chemosphere, 30 (1995) 243–256.

[24] D. Singh, D. Rupainwar, G. Prasad, K. Jayaprakas, Studies on the Cd (II) removal from water by adsorption, J. Hazard. Mater., 60 (1998) 29–40.

[25] KY. Foo, BH. Hameed, Insights into the modeling of adsorption isotherm systems, Chem. Eng. J., 156(1) (2010) 2–10.

[26] AE. Ofomaja, Y-S. Ho, Equilibrium sorption of anionic dye from aqueous solution by palm kernel fibre as sorbent, Dyes Pigm., 74(1) (2007) 60–66.

[27] G. Crini, HN. Peindy, F. Gimbert, C. Robert, Removal of C.I. basic green 4 (malachite green) from aqueous solutions by adsorption using cyclodextrin-based adsorbent: kinetic and equilibrium studies, Sep. Purif. Technol., 53(1) (2007) 97–110.

[28] A.S. Ozcan, K.O. Gö, A. Ozcan, Adsorption of lead (II) ions onto 8 hydroxyquinoline-immobilized Bentonite, J. Hazard. Mater., 161 (2009) 499–509.

[29] I.D. Mall, V.C. Srivastava, N.K. Agarwall, I.M. Mishra, Removal of Congo Red from aqueous solution by bagasse fly ash and activated carbon: Kinetic study and equilibrium isotherm analysis, Chemosphere, 61 (2005) 492–501.

[30] J.P. Hobson, Physical adsorption isotherms extending from ultra-high vacuum to vapor pressure, Phys. Chem., 73 (1969) 2720–2727.

[31] M. Dogan, M. Alkan, O. DemIRbas, Y. OzdemIR, C. Ozmetin, Adsorption kinetics of maxilon blue GRL onto sepiolite from aqueous solution, Chem. Eng., 124 (2006) 89–101.

[32] A.R. Khan, I.R. AlWaheab, A.A. Al-Haddad, Generalized equation for adsorption isotherms for multicomponent organic pollutants in dilute aqueous solution, Environ. Technol., 194 (1997) 13–23.

[33] R.A. Koble, T.E. Corrigan, Adsorption isotherms for pure hydrocarbons, Ind. Eng. Chem., 44 (1952) 383–387.

[34] B. Subramanyam, A. Das, Linearized and non-linearized isotherm models comparative study on adsorption of aqueous phenol solution in soil, Int. J. Environ. Sci. Technol., 6 (2009) 633–640.

[35] R. Han, J. Zhang, P. Han, Y. Wang, Z. Zhao, M. Tang, Study of equilibrium, kinetic and thermodynamic parameters about methylene blue adsorption onto natural zeolite, Chem. Eng. J., 145 (2009) 496–504.

[36] A. Günay, E. Arslankaya, I. Tosun, Lead removal from aqueous solution by natural and pretreated clinoptilolite: adsorption equilibrium and kinetics, J. Hazard. Mater., 146 (2007) 362–371.

[37] J. Toth, State Equations of the Solid-Gas Interphase Layers, ActaChim. Acad. Sci. Hung., 69 (1971) 311–328.

[38] V.C. Srivastava, I.D. Mall, I. M. Mishra, Equilibrium modelling of single and binary adsorption of cadmium and nickel onto bagasse fly ash, Chem. Eng. J., 117 (2006) 79–91.

[39] V.C. Srivastava, I.D. Mall, I. M. Mishra, Competitive adsorption of cadmium (II) and nickel (II) metal ions from aqueous solution onto rice husk ash, Chem. Eng.Process., 48 (2009) 370–379.

[40] S. Wang, Y. Dong, M. He, L. Chen, X. Yu, Characterization of GMZ bentonite and its application in the adsorption of Pb (II) from aqueous solutions, Appl. Clay Sci., 43(2) (2009) 164–171.

[41] P. Prasad, Shiva K. Prasad, V. Krishna Chaitanya, E. Babu, B. Sreedhar, S. Ramana Murthy, In situ FTIR study on the dehydration of natural goethite, J. Asian Earth Sci., 27 (2006) 503–511.

[42] R. Vempati, R. Loeppert, H. Sittertz-Bhatkar, R. Burghardt, Infrared vibrations of hematite formed from aqueous-and dry-thermal incubation of Si-containing ferrihydrite, Clays Clay Miner., 38 (1990) 294–298.

[43] RRUFF Project website (2015) Hematite. The RRUFF Project website containing an integrated database of Raman spectra, X-ray diffraction and chemistry data for minerals. http://rruff.info/Hematite

[44] N.S. Ahmedzeki, Adsorption filtration technology using iron-coated sand for the removal of lead and cadmium ions from aquatic solutions, Desal. Wat. Treat., 51 (2013) 5559–5565.

[45] X.S. Wang, H. H. Miao, W. He, H. L. Shen, Competitive adsorption of Pb (II), Cu (II), and Cd (II) ions on wheat-residue derived black carbon, J. Chem. Eng. Data, 56 (2011) 444–449.

[46] Y.G. Chen, W.M. Ye, X.M. Yang, F.Y. Deng, Y. He, Effect of contact time, pH, and ionic strength on Cd (II) adsorption from aqueous solution onto bentonite from Gaomiaozi, China. Environ. Earth Sci., 64 (2011) 329–336.

[47] R. Dianati-Tilaki, A. Mahvi, M. Shariat, S. Nasseri, Study of cadmium removal from environmental water by biofilm covered granular activated carbon, Iranian Journal of Public Health, 33 (2004) 43–52.
[48] F. Zhao, W.Z. Tang, D. Zhao, Y. Meng, D. Yin, M. Sillanpää, Adsorption kinetics, isotherms and mechanisms of Cd (II), Pb (II), Co (II) and Ni (II) by a modified magnetic polyacrylamide microcomposite adsorbent, J. Water Process Eng., 4 (2014) 47–57.
[49] V.C. Srivastava, I.D. Mall, I.M. Mishra, Antagonistic competitive equilibrium modeling for the adsorption of ternary metal ion mixtures from aqueous solution onto bagasse fly ash, Ind. Eng. Chem. Res., 47 (2008) 3129–3137.
[50] Y. Wu, Y. Wen, J. Zhou, J. Cao, Y. Jin, Y. Wu, Comparative and competitive adsorption of Cr (VI), As (III), and Ni (II) onto coconut charcoal, Environ. Sci. Pollut. Res., 20 (2013) 2210–2219.
[51] M. Vidal, M. J. Santos, T. Abrão, J. Rodríguez, A. Rigol, Modeling competitive metal sorption in a mineral soil, Geoderma, 149 (2009) 189–198.
[52] H. Merrikhpour, M. Jalali, Comparative and competitive adsorption of cadmium, copper, nickel, and lead ions by Iranian natural zeolite, Clean Technol. Envir., 15(2013) 303–316.
[53] C. Mahamadi, T. Nharingo, Competitive adsorption of Pb^{2+}, Cd^{2+} and Zn^{2+} ions onto Eichhorniacrassipes in binary and ternary systems, Bioresour. Technol., 101 (2010) 859–864.
[54] D. Kumar, A. Singh, J. Gaur, Mono-component versus binary isotherm models for Cu (II) and Pb (II) sorption from binary metal solution by the green alga Pithophoraoedogonia, Bioresour. Technol., 99 (2008) 8280–8287.